Int. J. Electrochem. Sci., 9 **(2014)** 4384 - 4393

International Journal of
ELECTROCHEMICAL
SCIENCE
www.electrochemsci.org

Ni-P-TiO_2 Composite Coatings on Copper Produced by Sol-Enhanced Electroplating

Yuxin Wang[1,2], Weiwei Chen[1], Abdul Shakoor[3], Ramazan Kahraman[3], Wei Lu[2], Biao Yan[2], Wei Gao[1]

[1] Department of chemical & Materials Engineering, the University of Auckland, PB 92019, Auckland 1142, New Zealand
[2] School of Materials Science and Engineering, Tongji University, Shanghai 200092, China
[3] Department of Chemical Engineering, College of Engineering, Qatar University, P. O. Box 2713, Doha, Qatar
*E-mail: ywan943@aucklanduni.ac.nz

Received: 7 February 2014 / *Accepted:* 10 March 2014 / *Published:* 19 May 2014

Ni-P-TiO_2 composite coatings were prepared on copper substrate by TiO_2 sol-enhanced electroplating. A systematic study of Ni-P-X coatings with different sol concentrations (TiO_2 concentration X from 0 to 50 mL/L) has been conducted in order to understand the effect of TiO_2 sol addition and the strengthening mechanism. The sol-enhanced coatings show significantly improved mechanical properties comparing with the traditional composite coatings. The optimal mechanical properties can be achieved when the sol concentration is 12.5 mL/L. In this case, the microhardness of Ni-P-12.5 mL/L TiO_2 composite coatings can reach ~710 HV while the Ni-P is ~520 HV. It is observed that the TiO_2 nanoparticles tend to aggregate and the voids may emerge in the coatings when excess sol was added into the electrolyte, decreasing the dispersion strengthen effect. Correspondingly, the mechanical property of Ni-P-50 ml/L TiO_2 coating declined.

Keywords: Sol-enhanced electroplating; Ni-P-TiO_2 composite coatings; Microhardness; Wear resistance

1. INTRODUCTION

Ni-P composite coatings are widely used in automobiles manufacturing, aviation, chemical processes and other industries due to their excellent properties such as high hardness, good wear and corrosion resistance [1-5]. Recently, there is a considerable interest in co-depositing superfine/nanoparticles as a second phase in electroplating and electroless Ni-P coatings [6-12]. It is demonstrated that the properties of Ni-P coatings can be enhanced by the highly dispersed

nanoparticles. Much attempt was made to achieve good dispersion of the nanoparticles. However, it is difficult for nanoparticles to achieve a good suspension as the large surface area and high surface energy tend to cause agglomeration of nanoparticles in electrolyte and composite coatings.

Sol-gel process has been widely applied to prepare uniform nanoparticles [13-15]. Recently, we have developed a novel technique: sol-enhanced composite plating, to synthesize highly dispersive oxide nano-particle reinforced composite coatings [16-20]. In this new method, transparent sol solution containing desirable oxide components is directly introduced into the electrolyte solution at a controlled speed. There is no step of solid particle formation in the processing, therefore no particle agglomeration occurs. This method can lead to a highly dispersive distribution of TiO_2 nanoparticles in the coating, resulting in significantly improved mechanical properties.

Comparing with the electroless plating process, electroplating process shows a broader application prospect for it is easy to operate and the deposition rate can be controlled by adjusting the voltage or current [21]. The present work reports our recent work of synthesizing nanostructured Ni-P-TiO_2 composite coating by sol-enhanced electroplating.

2. EXPERIMENTAL

Table 1. Electroplating bath composition and plating parameters

Bath composition and plating parameters	Quantity
$NiSO_4 \cdot 6H_2O$	250 g/L
$NiCl_2 \cdot 6H_2O$	15 g/L
NaCl	15 g/L
H_3BO_3	30 g/L
H_3PO_4	6 g/L
$NaH_2PO_2 \cdot 6H_2O$	20 g/L
Temperature	70±2^oC
pH value	3±0.5
Time	30 min
TiO_2 sol	0-50 mL/L
Current	50 mA/cm^2
Stir speed	500 rpm

In the present study, both Ni-P and Ni-P-TiO_2 composite coatings were electroplated onto Cu substrates (20×20×3 mm^3). Cu substrates were mechanically polished using SiC paper to a grit of #1200, then degreased ultrasonically in acetone. Before electroplating, the specimens were pre-treated in an alkaline solution containing 50 g/L NaOH and 10 g/L $NaH_2PO_4 \cdot H_2O$ at 65^oC for 15 min, then activated in acid solution containing 20 g/L citric acid and 60 g/L ammonium citrate at room temperature for 20 s.

TiO_2 sol was prepared as follows [19, 22]: 8.68 ml of tetrabutylorthotitanate [$Ti(OBu)_4$] was dissolved into the mixture solution of 35 mL ethanol and 2.82 mL diethanolamine (DEA). After

magnetic stirring for 2 h, it was hydrolyzed by adding a mixture of 0.45 mL deionized water and 4.5 mL ethanol dropwise under magnetic stirring.

The electroplating system consists of a Cu sample as the cathode and a Ni plate as the anode. The bath composition and plating parameters are given in Table 1. During the experiment, TiO_2 sol addition (0-50 mL/L) was adjusted to achieve the best properties. For convenient description, we use Ni-P-X mL/L TiO_2 to represent the coatings with different concentration of TiO_2 sol addition.

The Vickers microhardness of coating surface was measured using a load of 100 g with a holding time of 15 s. The final value quoted for the hardness of a coating was the average of 5 measurements. The coating morphologies and composition were analyzed using a field emission scanning electron microscope (FESEM) with an energy dispersive spectroscopy (EDS) system. The phase structure of the coatings was characterized by X-ray diffraction (XRD) with Cu Kα radiation (V = 30 kV, I = 15 mA). Diffraction patterns were recorded in the 2θ range from 20 to 90° at a scanning rate of 1° min^{-1}.

The nanoindentation tests were used to measure the load-displacement relationship, providing useful information including Young's modulus and hardness [23,24]. The test was conducted with a prescribed load in contact with the specimen. As the load is applied, the depth of penetration is measured. The area of contact at full load is calculated by the depth of the impression and the angle or radius of the indenter. The hardness is calculated by dividing the load by the area of contact. Shape of the unloading curve provides a measure of elastic modulus.

The nanoindentation tests were conducted on a Nano Indenter XP (MTS). The surface roughness has a significant influence on both hardness and elastic modulus of coatings determined from the nanoindentation tests. In order to rule out the influence of surface quality, the indentation depth should be much greater than the size of surface roughness [25]. The surface roughness of original Ni-P-X coatings was measured to be 40-60 nm by SPM of Tribo Indenter (Hystron). Therefore, we use the original coating for nanoindentation tests. 10 indents were performed on original coating specimens to a peak depth of 2000 nm in the present work.

The wear property of coatings was tested using a micro-tribometer (Nanovea, USA) in air with room temperature of 25°C and relative humidity of about 50% under dry, non-lubricated conditions. All wear tests were performed under a load of 5 N, a sliding speed of 2 m/min and a contact radius of 6 mm for a total sliding distance of 100 m. The wear track images of the electroplating coatings were observed by a high-revolution optical microscope.

3. RESULTS AND DISCUSSION

3.1 Microhardnsss of the as-deposited Ni-P-TiO_2 composite coatings

The Vickers hardness values of the as-deposited Ni-P-TiO_2 composite coatings as a function of TiO_2 sol concentration in the plating bath are shown in Fig.1. It can be seen that the microhardness of coatings are enhanced and varied significantly with the concentration of TiO_2 sol. The microhardness of the traditional Ni-P coating was ~520 HV. Following with the increasing TiO_2 sol addition, the

microhardness of coatings increased gradually and peaked at ~710 HV when the TiO_2 sol concentration is 12.5 mL/L.

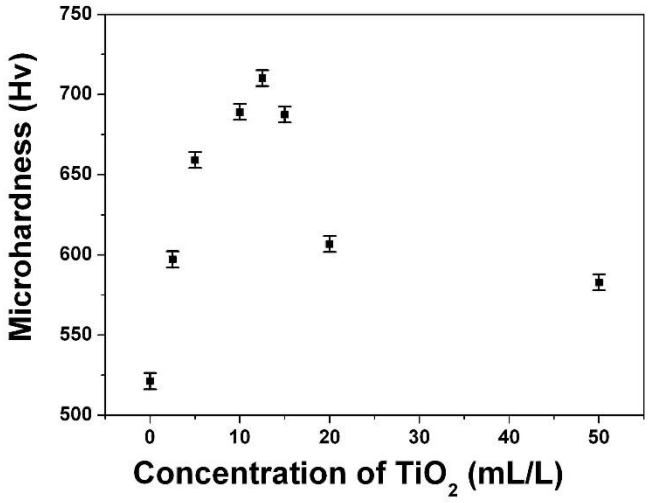

Figure 1. Effect of TiO_2 sol concentration on the microhardness of as-deposited Ni-P-TiO_2 composite coatings.

The enhancement of microhardness can be attributed to the incorporation of TiO_2 particles and microstructure change. According to the literature [26], more second-phase particles dispersion tends to have better mechanical properties of the composite coatings. However, our study indicated that higher concentrations of TiO_2 sol (>12.5 mL/L) lead to the decrease of microhardness. The microhardness of the Ni-P-50 mL/L TiO_2 composite coating reduces to ~580 HV, which is still higher than the pure Ni-P coating. The variation of microhardness can be attributed to the incorporation of TiO_2 nano-particles and microstructure change. In order to clarify the strengthening mechanism and the effect of sol concentration on the mechanical properties and microstructure, the coatings of Ni-P-X (X=0, 12.5, 50 mL/L TiO_2) were selected to investigate in the following parts.

3.2 Morphologies and phase structures of coatings

Figure 2 shows cross-section morphologies and a qualitative elemental distribution of coatings. The thickness of coatings was about the same at the level of 20 μm. A gleaming boundary between the coatings and the copper substrate is observed. No abruption or cracks were observed at the interfaces of the three coatings, evidence of a good adhesion between the copper substrate and coating.

For the traditional Ni-P coating (Fig. 2a), the P content is at a relatively high level of ~25 at.% evidenced by the EDS analysis. As TiO_2 content changes in the Ni-P coating, the elemental distribution of the as-plated coating varied. Ti element content of Ni-P-12.5 mL/L TiO_2 composite coating is at a low level of 0.12 at.%. No obvious TiO_2 particles were seen in the cross-section of coating which probably due to their small size and relatively low content (Fig. 2b). This result is consistent with our previous study in sol-enhanced electroless plating of Ni-P-TiO_2 [20,27]. Ni-P-

50mL/L TiO_2 composite coating contains higher Ti element content. However, with increasing TiO_2 addition, the agglomerated TiO_2 particles can be clearly seen as shown in Fig. 2(c). In addition, many voids were observed in the coatings.

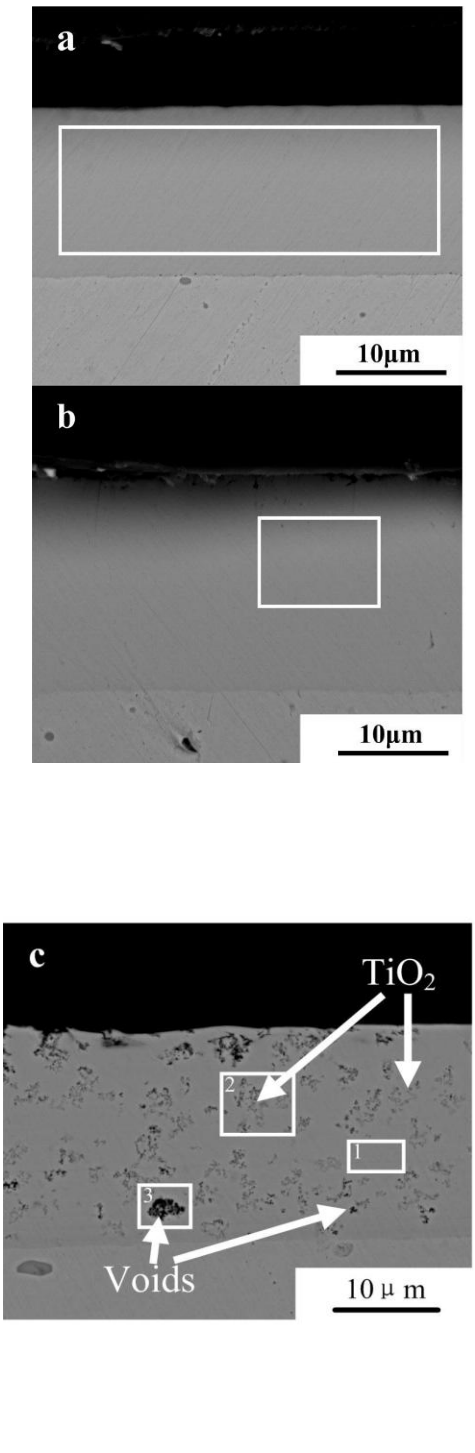

Element	Wt %	At %
P K	14.66	24.57
NiK	85.34	75.43
Total	100	100

Element	Wt %	At %
O K	0.41	1.39
P K	8.44	14.72
TiK	0.11	0.12
NiK	91.04	83.77
Total	100	100

1

Element	Wt %	At %
O K	0.62	2.12
P K	6.6	11.62
TiK	0.16	0.19
NiK	92.62	86.08
Total	100	100

2

Element	Wt %	At %
O K	1.56	5.18
P K	7.2	12.33
TiK	0.17	0.19
NiK	91.07	82.3
Total	100	100

3

Element	Wt %	At %
O K	6.65	19.34
P K	9.09	13.66
TiK	1.22	1.19
NiK	83.04	65.81
Total	100	100

Figure 2. Cross-sectional morphologies of the coatings and EDS elemental distribution of electroplating coatings: (a) traditional Ni-P coating, (b) Ni-P-12.5 mL/L TiO_2 composite coating, and (c) Ni-P-50 mL/L TiO_2 composite coating.

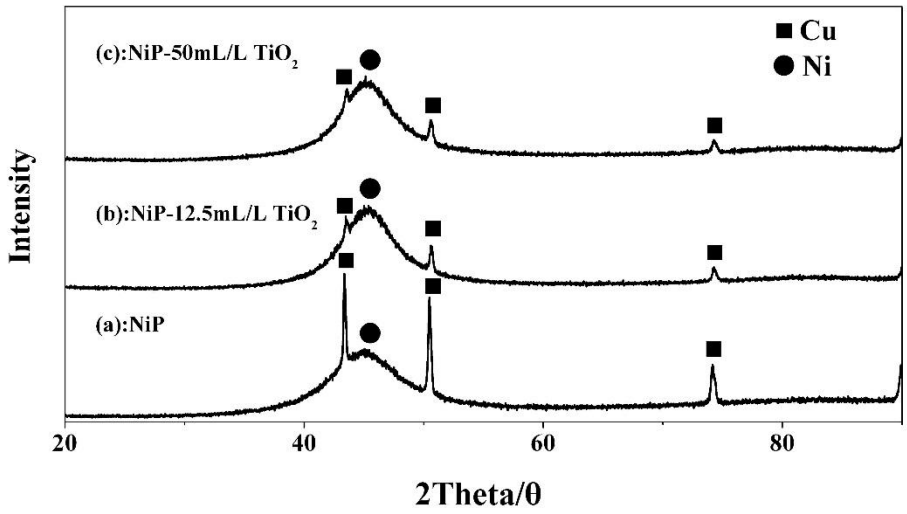

Figure 3. XRD spectra of coatings: (a) traditional Ni-P coating, (b) Ni-P-12.5 mL/L TiO_2 composite coating, and (c) Ni-P-50 mL/L TiO_2 composite coating.

The XRD patterns of coatings are shown in Fig. 3. The amorphous Ni phase was observed in Ni-P and sol-enhanced Ni-P-TiO_2 coatings, indicating that the sol addition did not significantly change the phase structure of coatings. The characteristic peak of TiO_2 in the composite coatings was not observed in the XRD patterns, probably due to the low content of TiO_2 in the coatings.

3.3 Mechanical properties

3.3.1 Nanoindentation test

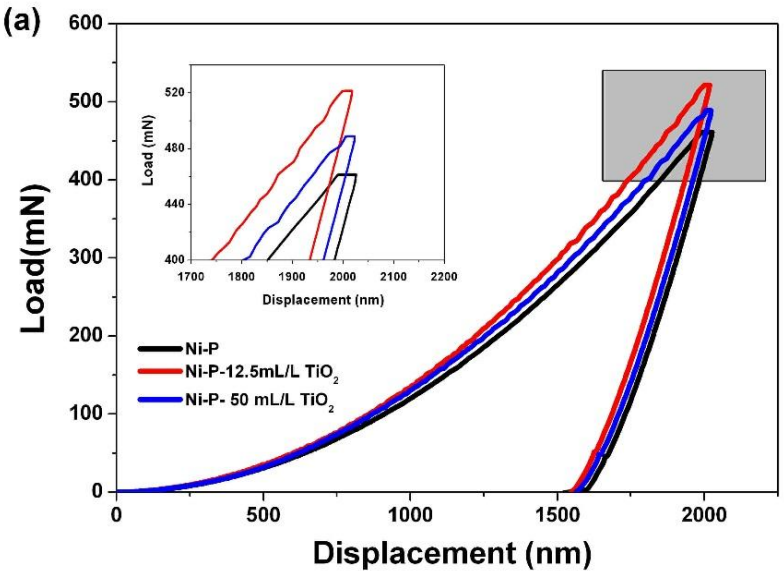

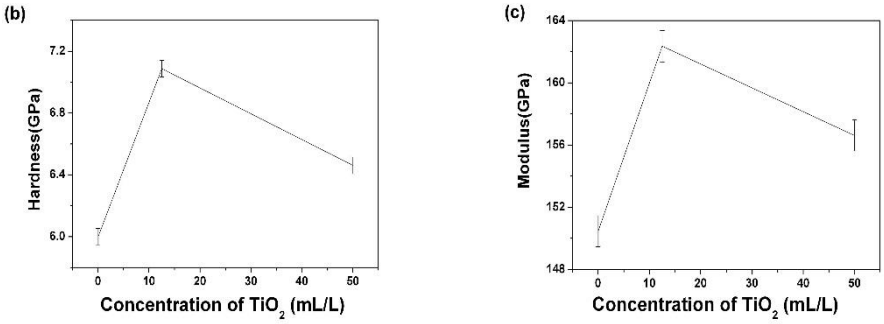

Figure 4. Nanoindentation results of coatings: (a) Load-displacement curves,(b) Nanoindentation hardness, (c) Elastic modulus.

Nanoindentation is a suitable technique to measure mechanical properties of nanostructured materials and thin coatings or films. Figure 4(a) shows the load-displacement curve for the coatings during 2000 nm deep indentation tests. The load applied in the same depth reveals the hardness and stiffness of coatings. The applied load for the sol-enhanced composite coatings (521 mN for 12.5 mL/L and 485 mN for 50 mL/L) is higher than that of Ni-P coating (455 mN). Figures 4b and 4c depict the hardness and elastic modulus of coatings calculated from the load-displacement curves, indicating that the results of nanoindentation tests have the same tendency as the microhardness shown in Fig. 1. The nanoindentation hardness and elastic modulus of sol-enhanced coatings were significantly improved compared with Ni-P coating. The improvement can be ascribed to the dispersion strengthening effect of the highly dispersive TiO_2 nanoparticles. However, further increment of TiO_2 sol addition above 12.5 mL/L led to a decrease of the dispersion strengthening effect as the agglomeration of TiO_2 particles were clearly observed in Fig.2(c). This can also explain that a high concentration of 50 mL/L TiO_2 sol reduces the nanoindentation hardness and elastic modulus (Fig. 4).

3.3.2 Wear resistance

Fig. 5 presents the friction coefficient of composite coatings with different TiO_2 sol additions. It can be seen that the friction coefficient of Ni-P coating started at 0.45 and maintained nearly over the full test process, which is perhaps due to its uniform microstructure and smooth surface. The Ni-P-12.5 mL/L TiO_2 composite coating has the lowest frication coefficient, which may be attributed to the highly dispersed TiO_2 nanoparticle in the Ni-P alloy matrix and excellent mechanical properties. The hard nano-scale particles embedded in composite coatings can reduce the direct contact between coating and abrasive surface. Furthermore, the well dispersed TiO_2 nanoparticles in the Ni-P matrix may have the effect of solid lubricants between the two wear surfaces, therefore reducing the friction coefficient.

The Ni-P-50 mL/L TiO_2 composite coating has a slightly higher friction coefficient than Ni-P coating between the sliding distances of 20-60 m. This is likely to be attributed to the TiO_2 particles agglomeration and voids emergence. Due to the reinforcement effect and self-lubrication of TiO_2

particles, the friction coefficient of Ni-P-50mL/L TiO_2 composite coating is lower than that of Ni-P coating during the sliding distances of 60-100 m.

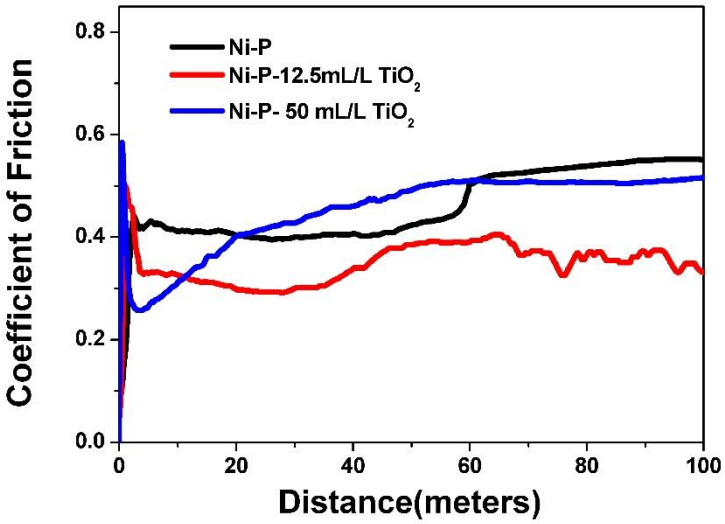

Figure 5. Frictional coefficient curve of coatings

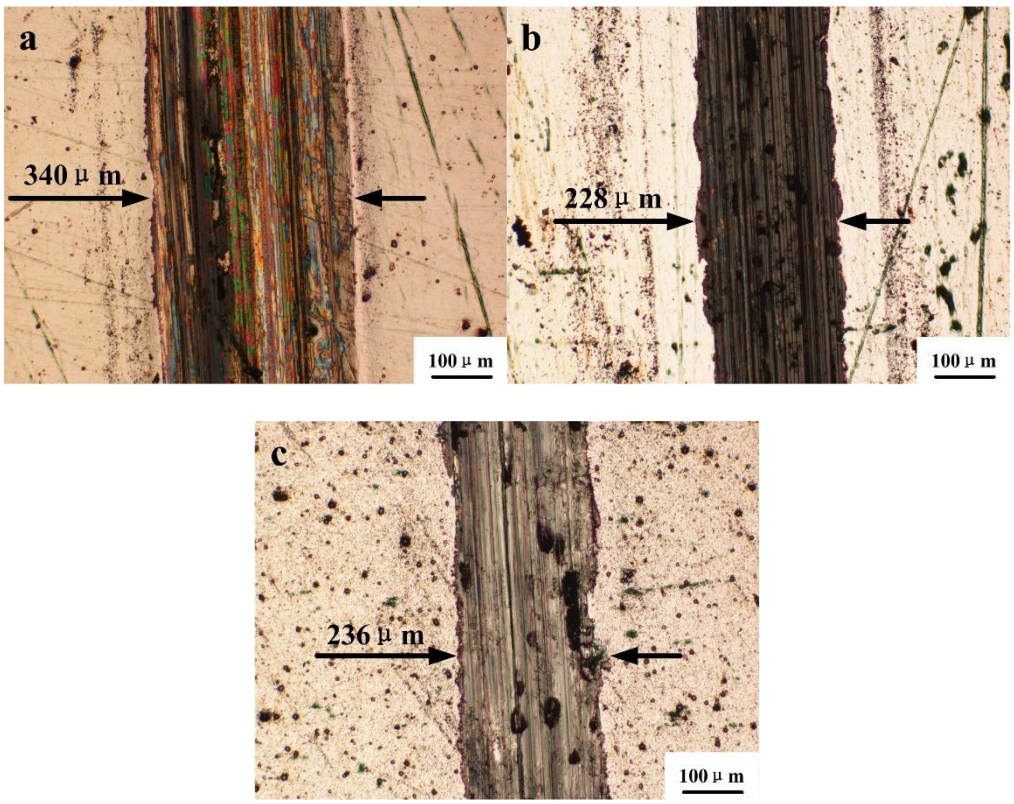

Figure 6. Wear track images of coatings: (a) traditional Ni-P coating, (b) Ni-P-12.5 mL/L TiO_2 composite coating, and (c) Ni-P-50 mL/L TiO_2 composite coating.

Fig. 6 shows the wear track images of Ni-P and Ni-P-TiO_2 coatings after a total sliding distance of 100 m. The wear track width of Ni-P coating was ~340 μm. It decreased to ~228 μm for the coating

with TiO_2 concentration of 12.5 mL/L, while the wear track width of Ni-P-50mL/L TiO_2 composite coating is ~236 μm. The width of wear track is a direct measure of the wear volume loss, and related to both the hardness and frictional coefficient of coatings.

4. CONCLUSIONS

Ni-P-TiO_2 composite coatings with a range of TiO_2 sol addition were prepared by electroplating method. Their mechanical properties including microhardness and wear resistance were studied. The microhardness of Ni-P-12.5 mL/L TiO_2 composite coatings can reach ~710 HV compared to ~520 HV of Ni-P coating, with increased Young's modulus and reduced friction coefficient. This improvement is attributed to the strengthening effect of TiO_2 dispersion in the Cu matrix. However, microstructure studies indicated that a higher concentration of 50 mL/L TiO_2 sol addition caused the agglomeration of TiO_2 particles and decreases the mechanical properties of the coatings. Further investigations are being carried out in an effort to apply this technology in real industrial applications.

ACKNOWLEDGEMENTS
The project is funded by NPRP grant # NPRP-4-662-2-249 from the Qatar National Research Fund (a member of Qatar Foundation). The related research is supported by a New Zealand Marsden Grant. The authors would like to thank the technical staff in Department of Chemical and Materials Engineering and the Research Centre for Surface and Materials Science for various assistances.

References

1. Q.J. Zhou, J.Y. He, J.X. Li, W.Y.Chu, L.J.Qiao, *Mater. Lett*. 60 (2006) 349.
2. M. Sarret, C. Müller, A. Amell, *Surf. Coat. Technol*. 201 (2006) 389.
3. K.H. Hou, M.C. Jeng, M. D. Ger, *Wear*. 262 (2007) 833.
4. M. Crobu, A. Scorciapino, B. Elsener, A. Rossi, *Electrochim. Acta*. 53 (2008) 3364.
5. X.T. Yuan, D. B. Sun, H. Y. Yu, H. M. Meng, *Appl. Surf. Sci*. 255 (2009) 3613.
6. J. Novakovic, P. Vassiliou, Kl. Samara, Th. Argyropoulos, *Surf. Coat. Technol*. 201 (2006) 895.
7. P. A. Gay, J. M. Limat, P. A. Steinmann, J. Pagetti, *Surf. Coat. Technol*. 202 (2007) 1167.
8. C.F. Malfatti, H.M. Veit, T.L. Menezes, J. Zoppas Ferreira, J. S. Rodrigues, J. -P. Bonino, *Surf. Coat. Technol*. 201 (2007) 6318.
9. Y. d. Hazan, D. Zimmermann, M. Z'graggen, S. Roos, C. Aneziris, H. Bollier, P. Fehr, T. Graule, *Surf. Coat. Technol*. 204 (2010) 3464.
10. F. Bigdeli, S. R. Allahkaram, *Mater. Design*. 30 (2009) 4450.
11. T. Rabizadeh, S. R. Allahkaram, *Mater. Design*. 32 (2011) 133.
12. J. Alexis, B. Etcheverry, J.D. Beguin, et. al, *Mater. Chem. Phys*. 120 (2010) 244.
13. C. N. Chervin, B. J. Clapsaddle, H. W. Chiu, A.E. Gash, J.H. Satcher Jr., S.M. Kauzlarich, *Chem. Mater*. 18 (2006) 1928.
14. P.H. Chiu, C.J. Huang, Y.H. Wang. *J. Electrochem. Soc*.155 (2008) K183.
15. Q. L. Zhang, F. Wu, H. Yang, D. Zou, *J. Mater. Chem*.18 (2008) 5339.
16. W.W. Chen, W. Gao, *Electrochim. Acta*. 55 (2010) 6865.
17. W.W. Chen, Y.D. He, W. Gao, *Surf. Coat. Technol*. 204 (2010) 2487.
18. W.W. Chen, Y.D. He, W. Gao, *J. Electrochem. Soc*. 157 (2010) E122.

19. W.W. Chen, W. Gao, Plating or Coating Method for Producing Metal–Ceramic Coatings on a Substrate, A Provisional Patent, New Zealand (June 2009).
20. W.W. Chen, W. Gao, Y.D. He, *J. Sol-Gel. Sci. Technol*. 55 (2010) 187.
21. Arthur A. Tracton: Coatings materials and surface coatings (CRC Press, Boca Raton 2007).
22. J.J. Qiu, Z.G. Jin, Z.F. Liu, X.X. Liu, G.Q. Liu, W.B. Wu, X. Zhang, X. D. Gao, *Thin. Solid. Films*. 515 (2007) 2897.
23. W.C. Oliver, G.M. Pharr, *J. Mater. Res*. 7 (1992) 1564.
24. S.H. Cho, C.G. Kang, S.M. Lee, *Mater. Sci. Eng*. A. 488 (2008) 72.
25. W.G. Jiang, J.J.Su, X.Q.Feng, *Engng Fract. Mech*. 75 (2008) 4965.
26. F.Y. Hou, W. Wang, H.T. Guo, *Appl. Surf. Sci*. 252 (2006) 3812.
27. W.W. Chen, W. Gao, Y.D. He, *Surf. Coat. Technol*. 204 (2010) 2493.